The Impact of an Antireflux Catheter on Target Volume Particulate Distribution in Liver-Directed Embolotherapy: A Pilot Study

Alexander S. Pasciak, PhD, James H. McElmurray, MD, Austin C. Bourgeois, MD, R. Eric Heidel, PhD, and Yong C. Bradley, MD

ABSTRACT

Purpose: To determine if there are differences in hepatic distribution of embolic particles following infusion with a standard end-hole catheter versus an antireflux microcatheter.

Materials and Methods: This prospective study included nine patients (age, 48–86 y) enrolled for treatment of hepatocellular carcinoma (n = 6), liver-dominant metastatic disease (n = 2), or intrahepatic cholangiocarcinoma (n = 1) with resin yttrium-90 (^{90}Y) microspheres. Before ^{90}Y treatment, each patient received two same-day sequential lobar infusions of technetium 99m (^{99m}Tc) macroaggregated albumin (MAA) via a conventional end-hole catheter and an antireflux microcatheter positioned at the same location. Differences in technetium 99m–MAA distribution within tumor and nontarget sites were evaluated by single-photon emission computed tomography (SPECT) on a qualitative and semiquantitative basis. The antireflux microcatheter was used for the ensuing ^{90}Y treatment, with posttreatment ^{90}Y positron emission tomography/computed tomography to assess distribution of ^{90}Y microspheres.

Results: Decreases in hepatic nontarget embolization were found in all patients when the antireflux catheter was used. These decreases ranged from a factor of 0.11 to a factor of 0.76 (mean, 0.42; $\sigma = 0.19$), representing a 24%–89% reduction. Increased tumor deposition was also noted in all patients, ranging from a factor of 1.33 to a factor of 1.90 (mean, 1.68; $\sigma = 0.20$), representing a relative increase of 33%–90%. Both findings were statistically significant ($P < .05$).

Conclusions: Although this pilot study identified differences in the downstream distribution of embolic particles when the antireflux catheter was used, further investigation is needed to determine if these findings are reproducible in a larger patient cohort and, if so, whether they are associated with any clinical impact.

ABBREVIATIONS

FDG = [^{18}F]fluorodeoxyglucose, MAA = macroaggregated albumin, PET = positron emission tomography, ROI = region of interest, SPECT = single-photon emission computed tomography

From the Department of Radiology (A.S.P.), University of Tennessee Medical Center; and Departments of Radiology (A.S.P., J.H.M., A.C.B., Y.C.B.) and Biostatistics (R.E.H.), University of Tennessee Graduate School of Medicine, Knoxville, Tennessee. Received October 27, 2014; final revision received January 27, 2015; accepted January 28, 2015. Address correspondence to A.S.P., Department of Radiology, University of Tennessee Medical Center, 1924 Alcoa Highway, Knoxville, TN 37920; E-mail: alexander.pasciak@gmail.com

A.S.P., J.H.M., and Y.C.B. received partial funding for this research from Surefire Medical (Westminster, Colorado). Neither of the other authors has identified a conflict of interest.

J Vasc Interv Radiol 2015; 26:660–669

http://dx.doi.org/10.1016/j.jvir.2015.01.029

Radioembolization with the use of yttrium-90 (^{90}Y) microspheres has become a widely used treatment for liver-dominant metastatic cancer and primary hepatocellular carcinoma (1,2). As with any liver-directed embolotherapy, the utility of radioembolization rests on the delivery of sufficient treatment to the tumor to produce a therapeutic effect while sparing normal liver and extrahepatic tissues from excessive toxicity. In this context, one potential rare complication associated with radioembolization is gastrointestinal tract ulceration from extrahepatic nontarget embolization of radiation-sensitive tissues in the stomach or small intestine (3,4). If pretreatment angiograms indicate that nontarget embolization may be a risk, occlusion of the

right gastric and gastroduodenal arteries is often performed before radioembolization (5,6). Although incidence rates of gastrointestinal ulceration are very low, devices such as antireflux catheters have been introduced to reduce the likelihood of extrahepatic nontarget embolization by preventing retrograde flow (7–9) of microspheres into unprotected gastroenteric collateral vessels.

Although antireflux catheters are commonly marketed as safety devices, there is preliminary evidence suggesting that they may also alter the downstream distribution of therapies such as radioembolization. A recent study (7) showed increased penetration of tantalum microspheres distal to the site of infusion in a renal porcine model when an antireflux microcatheter was used. Although this finding shows promise, its reproducibility in human hepatic radioembolization in the setting of variable tumor neovascularity remain unexplored. In the present work, nuclear imaging was used to evaluate changes in microparticle distribution, particularly in distal tumor, during hepatic radioembolization with the use of an antireflux microcatheter.

MATERIALS AND METHODS

Serial Infusion Protocol

The protocol in this prospective trial was approved by the performing site's institutional review board. Informed consent was obtained from all study participants. Enrollment criteria included patients with unresectable liver cancer clinically referred for hepatic ^{90}Y radioembolization for on- and off-label treatment of their disease, with no sex or race restriction. Exclusion criteria included total bilirubin level $>$ 2.0 mg/dL, serum albumin level $<$ 3.0 g/dL, aspartate and alanine aminotransferase levels no greater than five times the normal level, life expectancy $<$ 12 weeks, or Eastern Cooperative Oncology Group performance status $>$ 2. Nine patients (age, 48–86 y) were enrolled for treatment of hepatocellular carcinoma (n = 6), liver-dominant metastatic disease (n = 2), or intrahepatic cholangiocarcinoma (n = 1). Median Model for End-stage Liver Disease score was 7 (range, 6–13), with five of nine patients classified as having Child–Pugh class A cirrhosis and none classified as having class C cirrhosis. Segmental tumor-associated portal vein thrombus was present in one patient, and two patients had received transarterial chemoembolization greater than 6 months earlier. Mean tumor diameter was 7.9 cm (range, 3.8–14.6 cm), and the mean percentage tumor involvement in the treated lobe was 30% (range, 9%–61%). Additional demographic data are shown in **Table 1**.

Serial low-particulate infusions of technetium-99m (^{99m}Tc) macroaggregated albumin (MAA) were performed on the same day, in the same patient, and at the same point of infusion, with the only difference being the microcatheter used: a conventional end-hole microcatheter or an antireflux microcatheter (Surefire Infusion System; Surefire

Table 1. Description of Patients and Treatment

Pt. No.	Involved Lobe, Disease Origin	MAA Infusion Order	Relative MAA Change*		Treated Lobe Volume (cm^3)		Primary Lesion Tumor Diameter (cm)	^{90}Y Dose (MBq)		^{90}Y Treatment Endpoint
			Tumor ROI	Normal Liver ROI	Total	Disease		Prescribed	Delivered	
1	Right, colorectal	AR, EH	1.75	0.65	863	232	3.8	1,143	1,169	Air-phase
2	Left, cholangiocarcinoma	AR, EH	1.33	0.45	776	152	5.5	914	921	Air-phase
3	Right, breast	AR, EH	1.56	0.11	845	80	5.3	1,173	1,047	Air-phase
4	Left, HCC	AR, EH	1.90	0.22	730	236	8.4	1,010	1,084	Air-phase
5	Right, HCC	AR, EH	1.45	0.48	2,967	1,640	14.6	2,150	2,220	Air-phase
6	Right, HCC	EH, AR	1.67	0.37	2,226	540	9.9	1,869	1,939	Air-phase
7	Right, HCC	EH, AR	1.84	0.38	2,100	600	10.1	1,832	1,861	Air-phase
8	Right, HCC	EH, AR	1.85	0.76	1,275	785	6.6	Not treated		NA
9	Right, HCC	EH, AR	1.77	0.40	1,272	177	6.9	1,321	1,480	Air-phase

AR = antireflux microcatheter, EH = end-hole microcatheter, HCC = hepatocellular carcinoma, MAA = macroaggregated albumin, NA = not applicable, ROI = region of interest, ^{90}Y = Yttrium-90.

*Change relative to end-hole catheter: a value of 1 represents no change, a value of $>$ 1 indicates increased deposition with the antireflux catheter, and a value of $<$ 1 indicates decreased deposition with the antireflux catheter.

Medical, Westminster, Colorado). The same interventional radiologist (J.H.M.) administered all MAA doses to each patient from a 5 mL syringe (3 mL volume) in small aliquots using a push-pause infusion technique. One MAA infusion was performed using a 2.8-F Progreat end-hole microcatheter positioned at the expected future treatment location, whereas the other infusion used a 3-F antireflux microcatheter positioned at the same location. Single-photon emission computed tomography (SPECT) imaging was performed immediately following each infusion on a Symbia S SPECT system (Siemens, Bad Neustadt an der Saale, Germany) with a 128 × 128 × 128 matrix size, iterative reconstruction, and a body contouring orbit. The scan time was varied based on the injected activity to obtain acceptable image quality (Fig 1). The elapsed time between SPECT imaging of the same-day serial MAA infusions ranged from 192 to 286 minutes (mean, 238 min).

Because this protocol included same-day serial infusion of ^{99m}Tc MAA, residual MAA from the first infusion may have persisted at the time the second infusion was imaged. To minimize error associated with persistent activity, a technique commonly used in same-day renal (10) and cardiac perfusion (11) studies was applied. The first ^{99m}Tc MAA infusion had a mean

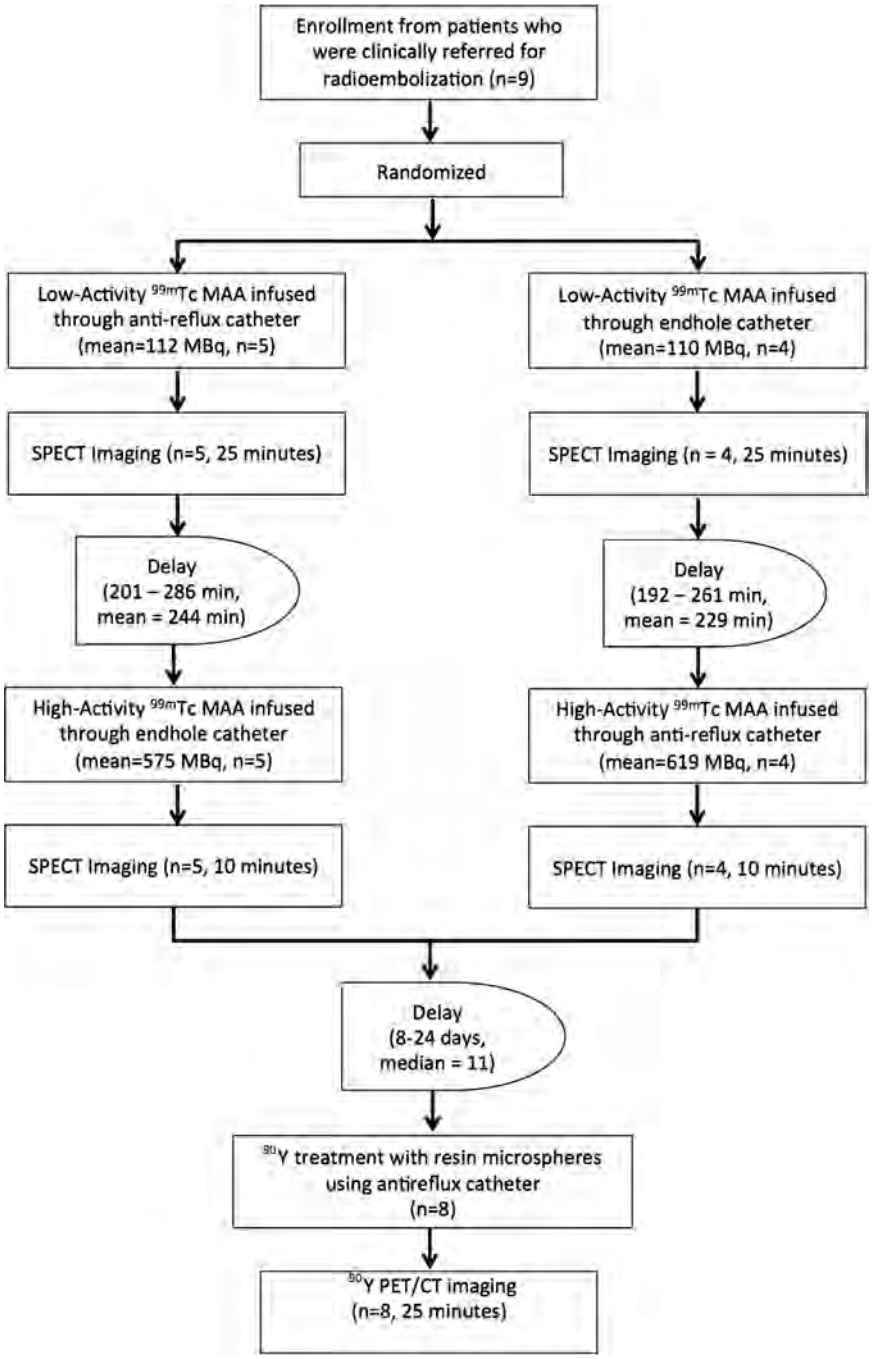

Figure 1. Flowchart describing the dual-infusion protocol used to compare antireflux and end-hole microcatheters.

activity of 111 MBq (range, 99–128 MBq), whereas the second had a mean activity of 595 MBq (range, 530–650 MBq). Considering only physical decay of ^{99m}Tc from the first to the second infusion, the maximum residual activity from the first infusion was less than 15% of the activity injected in the second infusion. A 15% residual activity represents a worst case for the study at the shortest interprocedural delay used, 192 minutes (Fig 1).

Another potential concern was alteration of vascular flow into the tumor compartment resulting from residual embolic particles from the first ^{99m}Tc MAA infusion at the time the second infusion was administered. This was mitigated by use of low-particulate dosages of less than 40,000 particles for infusion 1 and less than 200,000 particles for infusion 2. A nonrandomized 2 × 2 crossover design was used, with the initial five study patients receiving the first ^{99m}Tc MAA infusion with the antireflux microcatheter and the second infusion with the end-hole microcatheter. The catheter order was reversed in the remaining study subjects.

Treatment Protocol

Each study participant was treated with resin ^{90}Y radioembolization via the antireflux microcatheter (Fig 1). Catheter positioning was verified to be identical to that used during the ^{99m}Tc MAA infusions. The same push-pause infusion technique used for the MAA infusions was also used for the radioembolization delivery. Resin microsphere treatment dosage was determined according to the manufacturer-recommended body surface area treatment planning model (12). Following treatment, a liver-only ^{90}Y positron emission tomography/computed tomography (PET/CT) scan was performed on a Biograph mCT PET/CT scanner (Siemens) with the following scan parameters: time of flight, point-spread function resolution recovery, ordered-subset expectation maximization reconstruction with one iteration and 21 subsets, continuous bed motion at 0.2 mm/s, and a 400 × 400 matrix size. A detailed review of ^{90}Y PET/CT is provided elsewhere (13).

Nuclear Image Analysis

A board-certified nuclear medicine radiologist (Y.C.B.) reviewed the SPECT images from both infusions of MAA, blinded to which catheter was used. Pretreatment contrast-enhanced hepatic CT, [^{18}F]fluorodeoxyglucose (FDG) PET/CT, or hepatic-protocol magnetic resonance (MR) images were used to identify regions of tumor distal to the catheter position (ie, downstream) in the treated lobe. This distal region of interest (ROI) placement was selected based on previously reported results with the use of the antireflux catheter (7). One or more identically placed spherical ROIs with a 2-cm maximum diameter were drawn on each SPECT scan on an XD3 workstation (Mirada Medical, Denver, Colorado), and the number of counts contributing to each region was recorded and averaged (Fig 2). These data were normalized by the decay-corrected calibrated activity of ^{99m}Tc administered for the infusion, as well as the total live scan time, so that results from both infusions could be directly compared in terms of a relative change in activity deposition in the tumor. As ROIs were drawn in the same location for each SPECT scan, these regions were subject to the same attenuation, and this variable was removed from the final answer, eliminating the need for attenuation-corrected images. Unfortunately, to eliminate influence from attenuation, this technique necessitated the use of a small ROI (< 2 cm) and required a segmented analysis. This method was based on widely used semiquantitative regional cardiac SPECT (14), and has been further vetted with a phantom study described later. The aforementioned process was repeated in areas of normal hepatic parenchyma in the treated lobe to assess changes in MAA deposition in normal liver.

Following treatment of the patient with the antireflux catheter, a board-certified nuclear medicine radiologist compared the ^{90}Y PET/CT scan with the ^{99m}Tc MAA SPECT performed following infusion with the antireflux catheter to confirm the validity of MAA as a resin microsphere surrogate for each case.

Phantom Validation

A cylindrical phantom with a diameter of 12 cm and a volume of 1,750 mL containing a peripheral cylindrical insert with a diameter of 4.5 cm and a volume of 300 mL was used to validate the quantification methodology (Fig 3). The phantom background and insert were filled four times with ^{99m}Tc with total activities mirroring the low and high MAA activities used in patients at two different known background and insert relative activity concentrations, 3.3:1 and 6.2:1. Four SPECT scans of the phantom were obtained with use of the same scan time, reconstruction parameters, and postacquisition analyses that were used in patient scans following the low-dose and high-dose administrations, respectively.

Statistical Analysis

Skewness and kurtosis statistics were used to assess the assumption of normality of difference scores for the within-subjects analyses. Paired t tests were used for comparisons of catheters. An α-value of 0.05 was used to assume statistical significance, and all analyses were conducted with SPSS software (version 21; IBM, Armonk, New York).

RESULTS

The results of the phantom verification of the methodology described are presented in Table 2. The maximum error in assessing the relative change in the known activity concentration of the phantom insert was 5.6%.

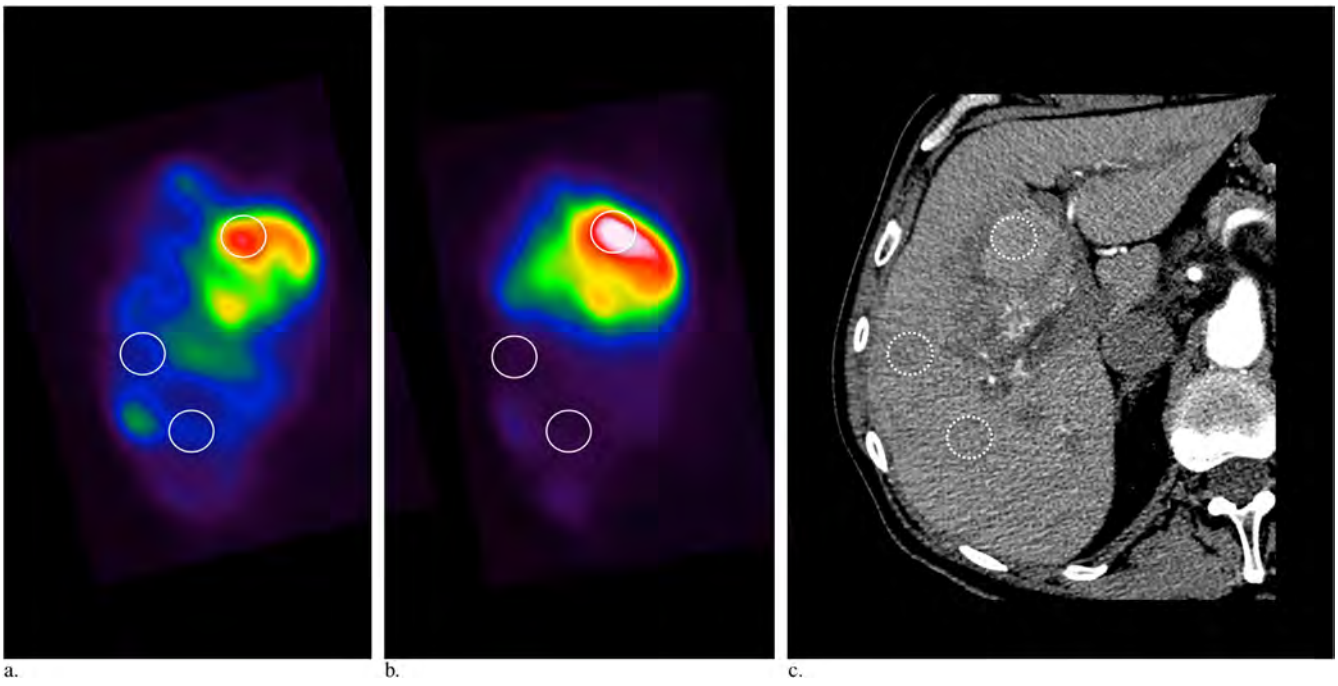

Figure 2. **(a)** Distribution of ^{99m}Tc MAA on axial SPECT following infusion with an end-hole catheter in a 73-year-old man with HCC (patient 9; Table 1). **(b)** Axial SPECT demonstrates the distribution of MAA following infusion with an antireflux catheter. **(c)** Pretreatment axial hepatic-protocol CT demonstrates a right-lobe hepatic mass. Example spherical 2-cm-diameter ROIs were used to measure changes in distal tumor and normal liver MAA uptake. Quantitative analysis showed changes in MAA deposition by a factor of 1.77 (77% increase) in distal tumor and a factor of 0.40 (60% decrease) in normal liver with the antireflux catheter.

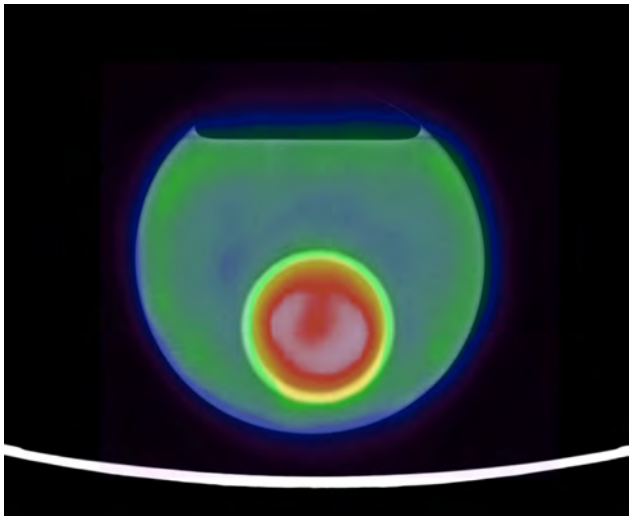

Figure 3. Fused SPECT and CT images from the phantom validation study with a 3.2:1 nominal insert-to-background activity concentration ratio. Fusion was performed on a Leonardo workstation (Siemens). Segmented phantom analysis with known activity concentrations resulted in a maximum error of 5.6% in the semiquantitative model used.

The maximum error in assessing the change in the phantom background was 3.5%.

Of the nine patients enrolled, eight completed the study, including radioembolization treatment and post-treatment ^{90}Y PET/CT imaging. However, as a result of escalation of liver-function test results between the MAA and treatment components of the study, one patient with HCC could not be treated. Identical catheter positioning was confirmed with archived images in all patients when using the end-hole and antireflux microcatheters for infusion of ^{99m}Tc MAA and the subsequent treatment with radioembolization (Fig 4).

In all nine patients, the ^{99m}Tc MAA same-day SPECT scans qualitatively revealed more uniform and extensive tumor coverage with greater relative activity deposition when the antireflux catheter was used. Semiquantitative analysis also revealed increases in MAA uptake in distal tumor in all nine patients. Consistent results were obtained regardless of tumor type and independent of pretreatment imaging obtained on contrast-enhanced CT, hepatic-protocol MR imaging, or FDG PET/CT used to reference the true tumor location (Figs 2, 5a–5c, 6a–6c).

Relative to the end-hole catheter, tumor ROI MAA deposition with the antireflux catheter changed by a factor ranging from 1.33 to 1.90 (mean, 1.68; $\sigma = 0.20$), which represents an increase in tumor deposition ranging from 33% to 90% when the antireflux catheter was used. This relative increase in deposition with the antireflux catheter was statistically significant ($P < .05$). The infusion order (end-hole catheter or antireflux catheter first), patient demographics, and relative change in MAA deposition distal to the site of infusion are shown in Table 1 for each study patient. There was no significant difference in the relative change in tumor

Table 2. Results from Experimental Phantom Study

Result	Measurement 1		Measurement 2	
	First Scan, Low Activity	Second Scan, High Activity	First Scan, Low Activity	Second Scan, High Activity
Injected total activity (MBq)	102.4	587.8	98.2	582.9
Injected relative insert:background activity concentration	3.3:1	6.2:1	6.2:1	3.3:1
Injected* relative change in activity concentration in phantom insert from first to second scan	–	1.45	–	0.69
SPECT† relative change in activity concentration in phantom insert from first to second scan	–	1.38	–	0.71
Percentage error, SPECT vs injected in phantom insert (%)	–	5.56	–	3.50
Injected relative change in activity concentration in phantom background from first to second scan	–	0.76	–	1.31
SPECT relative change in activity concentration in phantom background from first to second scan	–	0.78	–	1.36
Percentage error, SPECT vs injected in phantom background (%)	–	1.65	–	3.49

Note–Measurements performed by using single-photon emission CT with the same techniques used to analyze patient images are compared versus known phantom activity concentrations.
SPECT = single-photon emission computed tomography.
*Based on known decay-corrected quantities of radioactivity used to fill the phantom as measured using a Biodex Atomlab 100 Dose Calibrator.
†Performed by using identical corrections and measurement techniques as used in patient analysis.

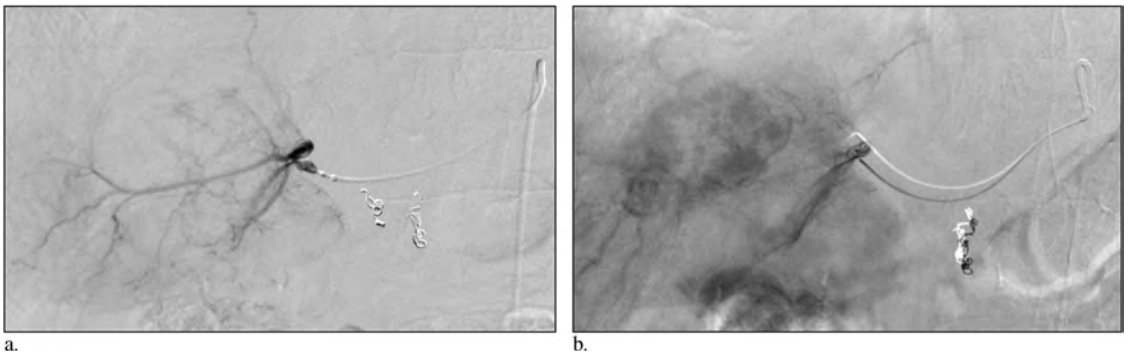

Figure 4. Archived digital subtraction angiographic images show catheter positioning for each infusion of ^{99m}Tc MAA before radioembolization treatment of a 73-year-old man with HCC (patient 9; Table 1): **(a)** antireflux catheter position and **(b)** end-hole catheter position are shown.

uptake ($P > .05$) when the order of infusion was varied, ie, when MAA was infused with the antireflux catheter first and the end-hole catheter second or with the end-hole catheter first and the antireflux catheter second.

In addition to increased tumor uptake, decreased MAA deposition in areas of normal (uninvolved) hepatic parenchyma in the treated lobe was qualitatively identified in all patients when the antireflux catheter was used (Figs 2, 6a–6c). Quantitative analysis indicated that, relative to the end-hole catheter, tumor ROI MAA deposition in areas of normal liver with use of the antireflux catheter quantitatively changed by a factor that ranged from 0.11 to 0.76 (mean, 0.42; $\sigma = 0.19$). This relative decrease in deposition in normal liver was statistically significant ($P < .05$). These results are summarized in Table 1.

Qualitative analysis of ^{90}Y PET data following treatment (Table 1) indicated excellent agreement between the distribution of radioembolization obtained by using the antireflux catheter and the distribution of MAA by using the antireflux catheter. In all eight patients, the distribution of MAA and ^{90}Y microspheres when the antireflux catheter was used closely matched pretreatment planning intentions (Figs 5b–5d, 6b–6d).

Complications

Among 17 embolizations performed by using the antireflux catheter (nine with ^{99m}Tc MAA, eight with resin microspheres), one infusion-related complication occurred. During infusion of ^{90}Y microspheres in the third study patient, the catheter occluded as a result of presumed clumping of microspheres and the procedure was halted. Nuclear medicine staff determined the percentage of the prescribed activity that was delivered before catheter occlusion. A new radioembolization

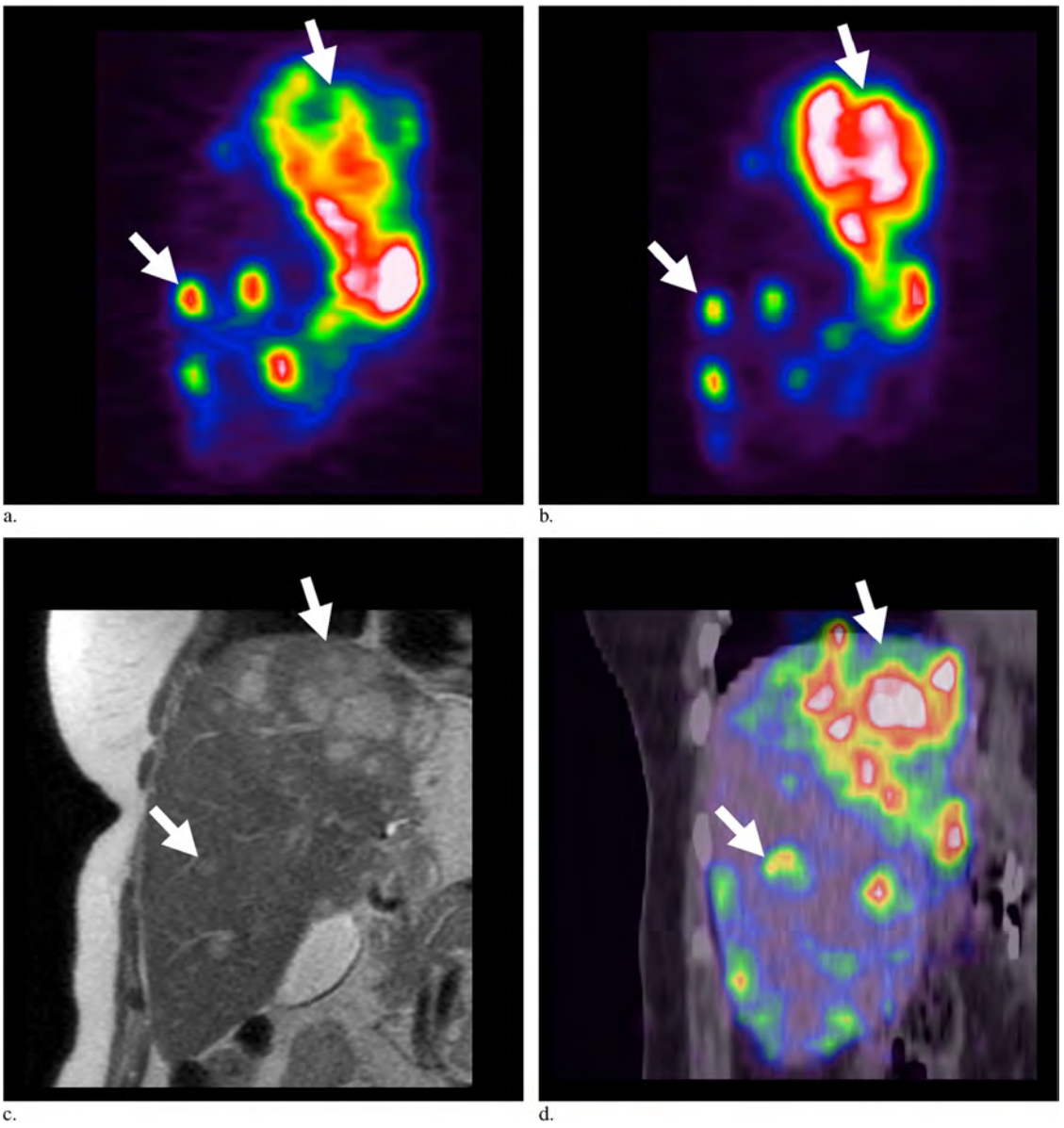

Figure 5. In all images, arrows indicate corresponding areas of disease on each image and imaging modality. **(a)** Distribution of ^{99m}Tc MAA on coronal SPECT following infusion with an end-hole catheter in a 48-year-old woman with HCC (patient 6; Table 1). **(b)** Coronal SPECT demonstrates the distribution of MAA following infusion with an antireflux catheter. **(c)** Pretreatment coronal hepatic protocol MR imaging demonstrates multicentric hepatic masses. **(d)** Posttreatment coronal ^{90}Y PET/CT following infusion of radioembolic materials with an antireflux catheter. Quantitative analysis showed a change in MAA deposition by a factor of 1.67 (67% increase) with the antireflux catheter in the large superior mass (top arrow).

treatment dosage was prepared that matched the undelivered portion of the original prescription, and this dosage was delivered on the same day by using a new antireflux catheter, without further incident.

DISCUSSION

In the present small patient series spanning a wide range of treatment indications and tumor sizes, the data suggest that the antireflux catheter altered the downstream distribution of embolic particles. In all study patients, more uniform tumor coverage and increases in MAA deposition in distal tumor were observed when the antireflux catheter was used. Consequently, nontarget embolization to normal liver in the treated lobe was also decreased with the use of the antireflux catheter. There are several different hypotheses describing possible mechanisms for these effects. Based on downstream arterial pressure measurements made with an antireflux catheter tip expanded, Rose et al (15) suggested that pressure decreases could create hepatopetal flow in downstream hepatoenteric collateral vessels, potentially resulting in distribution changes of radioembolization

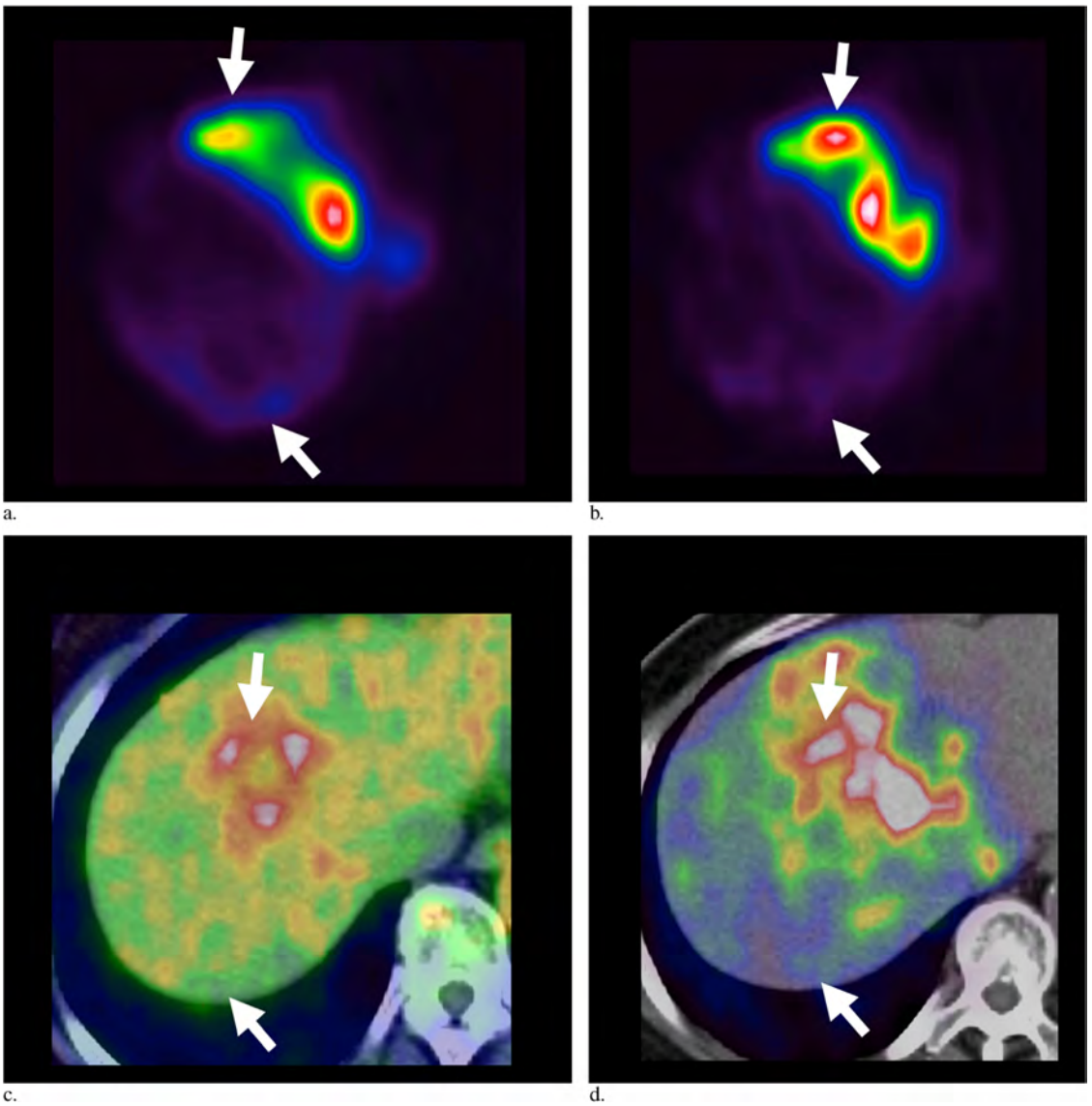

Figure 6. Arrows indicate corresponding areas on each image and imaging modality. **(a)** Distribution of ^{99m}Tc MAA on axial SPECT following infusion with an end-hole catheter in a 75-year-old woman with colorectal carcinoma metastases (patient 1; **Table 1**). **(b)** Axial SPECT demonstrates the distribution of MAA following infusion with an anti-reflux catheter. **(c)** Pretreatment axial FDG PET/CT demonstrates peripherally hypermetabolic right-lobe hepatic mass. **(d)** Posttreatment axial ^{90}Y PET/CT following infusion of radioembolization with an antireflux catheter. Quantitative analysis showed a change in MAA deposition by a factor of 1.75 (75% increase) with the antireflux catheter in the distal tumor in liver segment VIII (arrow). The lower arrow (segment VIII) indicates normal liver parenchyma that showed a change in MAA deposition by a factor of 0.65 (35% decrease) with the antireflux catheter.

and other liver-directed therapies. We propose that the results described in the present study can be more directly explained by the hypothesis that reduction in downstream pressure (15) with an antireflux microcatheter may result in vasoconstriction of the arteries and arterioles supplying normal liver tissue. At the same time, the structurally abnormal angiogenesis-induced tumor arterioles are not likely to vasoconstrict as a result of the absence of smooth muscle, innervation, and autoregulatory properties (16,17). This could preferentially shunt microspheres toward the tumor compartment, temporarily increasing the tumor-to-normal uptake ratio. Although this hypothesis has not been proven, it is congruent with similar findings with the use of intraarterial infusion of angiotensin II (18) or vasopressin (19).

The selection of infusion catheters for use in transcatheter liver-directed embolotherapy is largely dependent on operator preference, device familiarity, and empiric evidence. This is at least partially attributable to the absence of standardized performance data of catheters for the delivery of these therapies. The presented results provide evidence that a same-day, dual ^{99m}Tc MAA infusion protocol may be a valid tool to

evaluate the effect of different catheters on embolotherapy delivery. Because this method maintains the consistency of all variables other than the catheter, differences may be easy to identify in a small study cohort because subjects act as their own controls.

The validity of this technique rests on two assumptions, that (i) ^{99m}Tc MAA is an accurate surrogate for ^{90}Y microspheres and (ii) the embolic effects of the first MAA infusion do not appreciably alter the distribution of the second MAA infusion. Technetium 99m MAA represents the gold standard in pretreatment simulation of radioembolization and is a key component of the standard-of-care lung shunt evaluation integral in every ^{90}Y treatment (20). It is widely suggested that ^{99m}Tc MAA may be appropriate for the performance of pretreatment predictive dosimetry by using the partition model (21,22), and this technique is included as part of the ^{90}Y Medical Internal Radiation Dose Committee dosimetry equations (23). Posttreatment imaging with Bremsstrahlung SPECT (24) and ^{90}Y PET/CT (25) has also shown good agreement with pretreatment ^{99m}Tc MAA SPECT. In the present study, the validity of ^{99m}Tc MAA as a ^{90}Y microsphere surrogate was confirmed by the excellent qualitative agreement between the posttreatment ^{90}Y PET/CT and MAA infusions, both performed with the antireflux catheter.

Although no statistically significant differences were identified between patient subsets based on different MAA infusion orders, in view of the small sample size, the possibility of a type II error cannot be ignored. However, agreement between the distribution of ^{90}Y microspheres and MAA infused using an antireflux catheter and imaged with ^{90}Y PET/CT and ^{99m}Tc MAA SPECT, respectively, suggests that the embolic effect of the initial 40,000-particle MAA dose was insignificant. This is because a radioembolization treatment with resin microspheres can include anywhere from 8 million to 40 million microspheres in a typical dose (26). This embolic load is much higher than any MAA dose, but resin microspheres still mirrored the MAA distribution in these patients when the same infusion catheter was used.

The next step in this research is to validate these findings in a larger patient cohort to reduce the possibility of type I errors that may be present in these data. In addition, further efforts should be performed with the use of quantitative SPECT/CT, which would allow for a more robust, nonsegmented approach to the analysis of the postinfusion MAA images.

ACKNOWLEDGMENT

A portion of the technical component of this work was supported by the University of Tennessee Medical Center Molecular Imaging and Translational Research Program.

REFERENCES

1. Bilbao JI, Nag S, Reiser MF. Liver Radioembolization with 90Y Microspheres. New York: Springer Science & Business Media; 2009.
2. Salem R, Thurston KG. Radioembolization with 90Yttrium microspheres: a state-of-the-art brachytherapy treatment for primary and secondary liver malignancies. Part 1: Technical and methodologic considerations. JVIR 2006; 17:1251–1278.
3. Murthy R, Brown DB, Salem R, et al. Gastrointestinal complications associated with hepatic arterial yttrium-90 microsphere therapy. J Vasc Interv Radiol 2007; 18:553–561.
4. Riaz A, Lewandowski RJ, Kulik LM, et al. Complications following radioembolization with yttrium-90 microspheres:a comprehensive literature review. J Vasc Interv Radiol 2009; 20:1121–1130.
5. Covey AM, Brody LA, Maluccio MA, Getrajdman GI, Brown KT. Variant hepatic arterial anatomy revisited: digital subtraction angiography performed in 600 patients. Radiology 2002; 224:542–547.
6. Cosin O, Bilbao JI, Alvarez S, de Luis E, Alonso A, Martinez-Cuesta A. Right gastric artery embolization prior to treatment with yttrium-90 microspheres. Cardiovasc Intervent Radiol 2007; 30:98–103.
7. Arepally A, Chomas J, Kraitchman D, Hong K. Quantification and reduction of reflux during embolotherapy using an antireflux catheter and tantalum microspheres: *ex vivo* analysis. J Vasc Interv Radiol 2013; 24:575–580.
8. Fischman AM, Ward TJ, Patel RS, et al. Prospective, randomized study of coil embolization versus Surefire infusion system during yttrium-90 radioembolization with resin microspheres. J Vasc Interv Radiol 2014; 25: 1709–1716.
9. van den Hoven AF, Prince JF, Samim M, Arepally A, Zonnenberg BA, Zonneberg BA, et al. Posttreatment PET-CT-confirmed intrahepatic radioembolization performed without coil embolization, by using the antireflux Surefire Infusion System. Cardiovasc Intervent Radiol 2014; 37: 523–528.
10. Taylor AT, Fletcher JW, Nally JV, et al. Procedure guideline for diagnosis of renovascular hypertension. Society of Nuclear Medicine. J Nucl Med 1998; 39:1297–1302.
11. Husain SS. Myocardial perfusion imaging protocols: is there an ideal protocol? J Nucl Med Technol 2007; 35:3–9.
12. SIR-Spheres Yttrium-90 Resin Microspheres [package insert]. Lane Cove, Australia: Sirtex, 2012.
13. Pasciak AS, Bourgeois AC, McKinney JM, Chang TT, Osborne DR, Acuff SN, et al. Radioembolization and the Dynamic Role of (90)Y PET/CT. Front Oncol 2014; 4:38.
14. Salerno M, Beller GA. Noninvasive Assessment of Myocardial Perfusion. Circulation: Cardiovasc Imaging 2009; 2:412–424.
15. Rose SC, Kikolski SG, Chomas JE. Downstream hepatic arterial blood pressure changes caused by deployment of the surefire antireflux expandable tip. Cardiovasc Intervent Radiol 2013; 36:1262–1269.
16. Burke D, Davies MM, Zweit J, et al. Continuous angiotensin II infusion increases tumour: normal blood flow ratio in colo-rectal liver metastases. Br J Cancer 2001; 85:1640–1645.
17. Mattsson J, Appelgren L, Hamberger B, Peterson HI. Adrenergic innervation of tumour blood vessels. Cancer Lett 1977.
18. van den Hoven AF, Smits MLJ, Rosenbaum CENM, Verkooijen HM, van den Bosch MAAJ, Lam MGEH. The effect of intra-arterial angiotensin II on the hepatic tumor to non-tumor blood flow ratio for radioembolization: a systematic review. PLoS ONE 2014;9:e86394–e86394.
19. Durack JC, Hope TA, Seo Y, Saeed M, He J, Wilson MW, et al. Intravenous vasopressin for the prevention of nontarget gastrointestinal embolization during liver-directed cancer treatment: experimental study in a porcine model. J Vasc Interv Radiol 2012; 23:1505–1512.
20. Dezarn WA, Cessna JT, DeWerd LA, et al. Recommendations of the American Association of Physicists in Medicine on dosimetry, imaging, and quality assurance procedures for 90Y microsphere brachytherapy in the treatment of hepatic malignancies. Med Phys 2011; 38:4824–4845.
21. Ho S, Lau WY, Leung TW, Chan M, Ngar YK, Johnson PJ, et al. Partition model for estimating radiation doses from yttrium-90 microspheres in treating hepatic tumours. Eur J Nucl Med 1996; 23:947–952.
22. Ho SS, Lau WYW, Leung TWT, Chan MM, Johnson PJP, Li AKA. Clinical evaluation of the partition model for estimating radiation doses from yttrium-90 microspheres in the treatment of hepatic cancer. Eur J Nucl Med 1997; 24:293–298.
23. Gulec SAS, Mesoloras GG, Stabin MM. Dosimetric techniques in 90Y-microsphere therapy of liver cancer: The MIRD equations for dose calculations. J Nucl Med 2006; 47:1209–1211.

24. Knesaurek K, Machac J, Muzinic M, DaCosta M, Zhang Z, Heiba S. Quantitative comparison of yttrium-90 (90Y)-Microspheres and Technetium-99m (99mTc)-Macroaggregated Albumin SPECT Images for Planning 90Y Therapy of Liver Cancer. Technol Cancer Res Treat 2010; 9: 253–261.

25. Kao YH, Steinberg JD, Tay Y-S, et al. Post-radioembolization yttrium-90 PET/CT - part 2: dose-response and tumor predictive dosimetry for resin microspheres. EJNMMI Research 2013;3:1–1.

26. Kritzinger J, Klass D, Ho S, et al. Hepatic embolotherapy in interventional oncology: technology, techniques, and applications. Clin Radiol 2013; 68:1–15.